Tuning cellular uptake of nanoparticles via ligand density: Contribution of configurational entropy

Yudie Zhang,[1] Long Li,[1,2,*] and Jizeng Wang[1,†]

[1]*Key Laboratory of Mechanics on Disaster and Environment in Western China, Ministry of Education, College of Civil Engineering and Mechanics, Lanzhou University, Lanzhou, Gansu 730000, China*

[2]*PULS Group, Institute for Theoretical Physics, FAU Erlangen-Nürnberg, Erlangen 91058, Germany*

(Received 12 August 2019; revised 12 July 2020; accepted 25 October 2021; published 11 November 2021)

The bioactivity of nanoparticles (NPs) crucially depends on their ability to cross biological membranes. A fundamental understanding of cell-NP interaction is hence essential to improve the performance of the NP-based biomedical applications. Although extensive studies of cellular uptake have converged upon the idea that the uptake process is mainly regulated by the elastic deformation of the cell membrane or NP, recent experimental observations indicate the ligand density as another critical factor in modulating NP uptake into cells. In this study, we propose a theoretical model of the wrapping of an elastic vesicle NP by a finite lipid membrane to depict the relevant energetic and morphological evolutions during the wrapping process driven by forming receptor-ligand bonds. In this model, the deformations of the membrane and the vesicle NP are assumed to follow the continuum Canham-Helfrich framework, whereas the change of configurational entropy of receptors is described from statistical thermodynamics. Results show that the ligand density strongly affects the binding energy and configurational entropy of free receptors, thereby altering the morphology of the vesicle-membrane system in the steady wrapping state. For the wrapping process by the finite lipid membrane, we also find that there exists optimal ligand density for the maximum wrapping degree. These predictions are consistent with relevant experimental observations reported in the literature. We have further observed that there are transitions of various wrapping phases (no wrapping, partial wrapping, and full wrapping) in terms of ligand density, membrane tension, and molecular binding energy. In particular, the ligand and receptor shortage regimes for the small and high ligand density are, respectively, identified. These results may provide guidelines for the rational design of nanocarriers for drug delivery.

DOI: 10.1103/PhysRevE.104.054405

I. INTRODUCTION

Understanding the cellular uptake of nanoparticles (NPs) can greatly contribute to a wide range of applications concerning drug delivery, therapeutics, and biomedical diagnosis [1–6]. Specifically, it is worth mentioning that active targeting can be achieved, and drugs can be effectively absorbed in the targeting positions by regulating the physical, chemical, and geometrical properties of NPs. There have been growing research activities towards such understanding on biophysical factor dependent cellular uptake of NPs, such as size [7–10], geometry [11–16], orientation [8,11,17–19], stiffness [20–22], cytoskeleton deformation [23,24], and ligand pattern [25–28].

In most of the preceding studies, attention had been mainly focused on how elastic deformation may mediate the cellular uptake of NPs; very few works investigated the influence of ligand density on the cell-NP interactions, although experimental results do show that ligand density has a significant effect on such cellular uptake events [29–34]. Specially, Shen *et al.* [29] conducted experiments on wheat germ agglutinin (WGA) modified PEG-PLA NPs with different WGA/maleimide molar ratios targeting to Calu-3 cells. They observed that the highest efficiency of uptake is found when the molar ratio of WGA to maleimide is a characteristic value such as 1:10. Moreover, by applying expressed protein ligation click conjugation to enable NPs labeled with targeting affibodies at differing ligand densities, Elias *et al.* [30] examined the existence of a ligand density with intermediate value associated with the most effective cell targeting. To evaluate the effects of mannose density on *in vitro* and *in vivo* cellular uptake of polymeric NPs in macrophages, by synthesizing mannose-modified trimethyl chitosan-cysteine (MTC) conjugated with mannose densities of 4%, 13%, and 21% (MTC-4, MTC-13, and MTC-21), Chu *et al.* [32] observed that the uptake amounts of MTC-4 NPs are the highest for all NPs internalized into the macrophages. These experimental results clearly prove that cellular uptake of NPs can significantly depend on the ligand density.

In addition to the influences of ligand density and elastic deformation, the wrapping process during the uptake of NPs is also accompanied and influenced by the evolution of configurational entropy of adhesion molecules. For example, a vesicle binding to a rigid substrate has been found to be sensitive to the change of configurational entropy of distributed receptors [35]. It is further shown that the distributional entropy also plays a decisive role in the effective adhesion energy of two

*longl@lzu.edu.cn
†jzwang@lzu.edu.cn

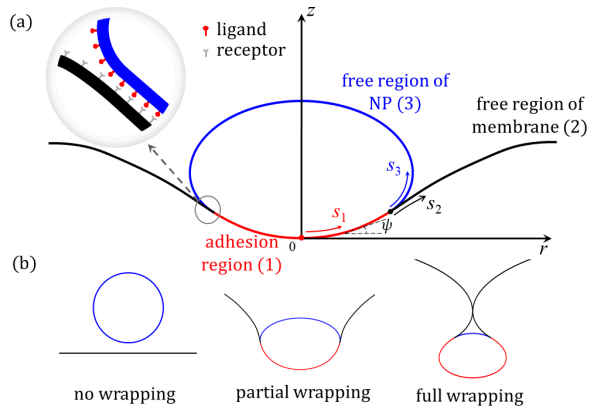

FIG. 1. (a) Schematic of the cellular uptake of deformable vesicle NP via receptor-ligand bonds. The system is divided into three parts: adhesion region, free region of membrane, and free region of NP. The circumference of the vesicle NP, the lengths of the adhesion region (red), and the free region (blue) are denoted as l_t, l_1, and l_3, respectively. The length of the free region on each side of the cell membrane is l_2. (b) Schematic for the states of no wrapping with zero adhesion length, partial wrapping in which the membrane is not closed around the NP, and full wrapping in which the encapsulation of the NP occurs.

identical opposing membranes interacting with each other through receptor-ligand bonds [36–38].

In spite of these theoretical and experimental advances, there remain grand challenges in quantitative description of behaviors of ligand density dependent cellular uptake of NPs, which involves the coupling between elastic deformation of the whole system, and statistical mechanics behavior of adhesion molecules.

In order to investigate how the ligand density may couple the elastic deformation to influence the wrapping process of NPs, in this study we will establish a theoretical model on the adhesive wrapping of a soft elastic vesicle NP by a finite lipid membrane via formation of receptor-ligand bonds. In this model, deformation of the vesicle NP and lipid membrane is assumed to follow the framework of continuum mechanics, whereas the configurational entropy of mobile receptors is described by statistical mechanics. Based on this model, we will systematically investigate how the ligand density may affect the morphology evolution, and what role will be played by the statistical mechanics behavior of receptors in the energetic evolution of the system during the adhesive wrapping.

II. MODEL

Figure 1 displays the two-dimensional (2D) problem where a NP uniformly coated with immobile ligands interacts with a finite lipid membrane embedded with free receptors. The NP is considered and modeled as a deformable 2D lipid vesicle with constant contour length $2l_t$.

The membrane can be viewed as an effective portion of a whole cell membrane involved in the wrapping of the vesicle NP. We denote the size of the lipid membrane for NP wrapping as $2l_m$. This assumption can be easily understood because when cells are infected by many viruses simultaneously, each virus will occupy a certain proportion of the cell membrane on average. The receptor resources required for the endocytosis of a virus will be roughly considered as being limited to the surrounding cell membrane due to competition with other viruses. In terms of this effective size for cell membrane, on one hand, we consider that this size is large enough comparing to that of the NP, so that the boundaries are unperturbed by the contact of a relatively small vesicle NP. On the other hand, we assume that, for this effective size of membrane, within the average timescale of virus uptake by cells, the farthest receptor should be just able to reach the contact area of the NP and membrane. Following these considerations, the ratio between this effective membrane size and NP size, $\lambda = l_m/l_t$, has been estimated at around 10 for a vesicle NP wrapped by an infinite membrane (see Appendix A for details).

Elastic deformations of both the membrane and vesicle NP can be described by the Canham-Helfrich theory [39,40]. Typically, the number density of ligands on the vesicle surface is larger than the receptors' density on the membrane. We assume that a receptor-ligand bond will be immediately and firmly formed once a diffusing receptor reaches the adhesion region of the membrane-NP system, so that there are no unbound receptors and ligands in the adhesion region. During the wrapping process, favorable receptor-ligand binding energy will be consumed by the elastic deformations of membrane and vesicle NP, and the change of configurational entropy of the distributed receptors. Consequently, the total free energy can be described as

$$E_{\text{tot}} = E_{el} + E_{en} + E_{ad}, \tag{1}$$

where E_{el}, E_{en}, and E_{ad} represent the elastic energy of the cell membrane and vesicle NP including bending and tension, the entropy contribution to the free energy, and NP–cell membrane adhesion energy, respectively.

The elastic energy of the cell membrane and vesicle NP can be given by the Canham-Helfrich theory as [39–44]

$$E_{el} = \sum_{i=1}^{3} \frac{\kappa_i}{2} \int_0^{l_i} \dot{\psi}_i^2 ds_i + \sum_{i=1,2} \sigma \int_0^{l_i} (1 - \cos\psi_i) ds_i, \tag{2}$$

where σ is the surface tension of the membrane; the subscripts 1, 2, and 3 stand for the three regions, namely, adhesion region, the free region of the membrane, and the free region of the NP; ψ_i, s_i, l_i, and κ_i are the tangent angle, arc length coordinate, total arc length, and bending stiffness of each region, respectively; the dot in the first term means the derivative with respect to the arc length. We also have $\kappa_1 = \kappa_m + \kappa_n$, $\kappa_2 = \kappa_m$, and $\kappa_3 = \kappa_n$, where κ_m and κ_n are the bending stiffness of the membrane and vesicle NP. The first term on the right side of Eq. (2) represents the bending energy of the vesicle NP and the membrane, and the second term represents the energy of tensile deformation of the membrane.

We assume that the ligands and receptors are of the same size, and there are S_T maximum permissible sites on the vesicle NP for the ligands. Correspondingly, the total number of active sites on the membrane for receptors can be expressed as λS_T. The dimensionless densities of ligands and receptors, ρ_L and ρ_R, are introduced to describe the extent of ligand and receptor coverage (e.g., for $\rho_L = 1$, the vesicle NP contains saturated ligand molecules on the surface, while for $\rho_L = 0$, there is no ligand on the vesicle NP surface). Based on the analysis of ligand density on HIV and the associated receptor

density on relevant cells, $\rho_R = 0.1$ is adopted in this study (see Appendix B for details).

All the possible configurations of the distributed receptors on the membrane are denoted as Ω, which can be counted as [45]

$$\Omega = \mathrm{C}^{\lambda S_T - \alpha S_T}_{\rho_R \lambda S_T - \rho_L \alpha S_T} \mathrm{C}^{\rho_L \alpha S_T}_{\rho_L \alpha S_T}, \tag{3}$$

where $\alpha = l_1/l_t$ is the wrapping degree, and $\mathrm{C}^n_m = \frac{n!}{m!(n-m)!}$ is the combination in mathematics. The first term on the right side of Eq. (3) expresses the number of possible configurations of free receptors distributed in the free region of the membrane. For the bounded receptors on the adhesion region, the number of distribution configurations is determined by the the second term on the right of Eq. (3), which is set to be 1 in this case.

Likewise, the number of all possible configurations of the distributed receptors before wrapping can be calculated as [45]

$$\Omega_0 = C^{\lambda S_T}_{\rho_R \lambda S_T}. \tag{4}$$

Then, the change of configurational entropy can be obtained as

$$\Delta S = k_B(\ln\Omega - \ln\Omega_0), \tag{5}$$

where k_B is the Boltzmann constant. Inserting Eqs. (3) and (4) into Eq. (5) and applying Stirling's approximation [45], Eq. (5) can be rewritten as

$$\begin{aligned}\frac{\Delta S}{k_B S_T} &= (\lambda-\alpha)\ln\frac{\lambda-\alpha}{(\lambda-\alpha)-(\lambda\rho_R-\alpha\rho_L)} \\ &+ (\lambda\rho_R-\alpha\rho_L)\ln\frac{(\lambda-\alpha)-(\lambda\rho_R-\alpha\rho_L)}{\lambda\rho_R-\alpha\rho_L} \\ &+ \lambda\rho_R\ln\frac{\rho_R}{1-\rho_R} + \lambda\ln(1-\rho_R).\end{aligned} \tag{6}$$

Once the change of entropy, ΔS, is known, the entropic part of the free energy can be determined by

$$E_{en} = -T\Delta S, \tag{7}$$

with the absolute temperature T.

Subsequently, the cell membrane-NP adhesion energy is described by

$$E_{ad} = -\alpha\rho_L S_T e_{RL}, \tag{8}$$

where $\alpha\rho_L S_T$ refers to the number density of receptor-ligand bonds and e_{RL} is the binding energy of each receptor-ligand bond.

To reflect the intrinsic effect of the parameters on the configuration of the system, dimensionless parameters are employed as follows [46,47]:

$$\begin{aligned}&\bar\sigma = \frac{\sigma R^2}{\kappa_m},\ \bar\kappa_n = \frac{\kappa_n}{\kappa_m},\ \bar\kappa_m = 1,\ \bar\gamma = \frac{k_B T S_T R}{\kappa_m}, \\ &\bar e_{RL} = \bar\gamma\frac{e_{RL}}{k_B T} = \frac{e_{RL} S_T R}{\kappa_m},\ \Delta\bar S = \frac{\Delta S}{k_B S_T},\end{aligned} \tag{9}$$

$$\begin{aligned}&\bar E_{el} = \frac{E_{el}R}{\kappa_m},\ \bar E_{en} = \frac{E_{en}R}{\kappa_m} = -\bar\gamma\Delta\bar S, \\ &\bar E_{ad} = \frac{E_{ad}R}{\kappa_m} = -\bar e_{RL}\alpha\rho_L,\ \bar E_{\mathrm{tot}} = \frac{E_{\mathrm{tot}}R}{\kappa_m},\end{aligned} \tag{10}$$

where $R = l_t/\pi$ is the effective radius of the NP, by which all lengths are scaled.

A technique of numerical optimization is employed to determine the minimum energy state of the wrapping process, and the corresponding configurations of both the vesicle NP and membrane. For this purpose, the tangential angles, ψ_i, $i = 1, 2, 3$, are approximated by a truncated Fourier series of corresponding arc lengths as [48–50]

$$\begin{aligned}&\psi_i(s_i) = \psi_0^{(i)} + \left(\psi_l^{(i)} - \psi_0^{(i)}\right)\frac{s_i}{l_i} + \sum_{j=1}^{N} a_j^{(i)} \sin\frac{\pi j s_i}{l_i} \\ &\text{for} \quad i = 1,\ 2,\ \text{and}\ 3,\end{aligned} \tag{11}$$

where $\psi_0^{(i)}$ and $\psi_l^{(i)}$ are the tangential angles at the boundaries $s_i = 0$ and $s_i = l_i$; N is the number of adopted Fourier modes, which is assumed to be sufficiently large to guarantee the satisfactory numerical accuracy; and $a_j^{(i)}$ are the corresponding unknown Fourier amplitudes. In the current context, we choose $N = 70$, after numerical verification on the convergence and accuracy. We set boundary conditions as $\psi_0^{(1)} = \psi_l^{(2)} = 0$, $\psi_l^{(3)} = \pi$, and $\int_0^{l_1}\cos\psi_1 ds_1 + \int_0^{l_3}\cos\psi_3 ds_3 = 0$. The continuity condition, $\psi_l^{(1)} = \psi_0^{(2)} = \psi_0^{(3)}$, should also be satisfied during the numerical simulation. As such, the equilibrium wrapping state can be obtained by minimizing the total energy with respect to the unknown Fourier amplitudes $a_j^{(i)}$ and wrapping degree α, based on the algorithm of sequential quadratic programming, simply listed as follows (please see Ref. [51] for details): (1) The current nonlinear optimization problem can be equivalent to a sequence of optimization subproblems by Taylor series expansion. (2) With initial values, we can solve these quadratic subproblems by applying the smooth Newton method with a sequence of iterations until the converged results are obtained.

We should note that the wrapping degree α can reach the maximum value of 1 as we have neglected the effect of the excluded volume of the membrane and allowed different sections of the membrane to cross each other. In order to distinguish the regime with membrane crossing from that without membrane crossing, we define a critical value of the wrapping degree, α_c, at which membranes on two sides of the wrapped vesicle NP just start to make contact. Obviously, in the regime $1 \geqslant \alpha > \alpha_c$ there will be membrane sections that pass through each other. We consider this regime as unphysical due to the neglect of the excluded volume effect. In reality, the contacted membrane sections will be subject to a fusion process to form an closed encapsulation in terms of different mechanisms.

III. RESULTS AND DISCUSSIONS

For a given ligand density, a wrapping state of minimum free energy should be reached. Figure 2 plots the variations of the dimensionless energy change $\Delta\bar E_{\mathrm{tot}} = \bar E_{\mathrm{tot}} - \bar E_{\mathrm{tot}}|_{\alpha=0}$; the wrapping degree α; and the dimensionless energy components $\bar E_{el}$, $\bar E_{en}$, $\bar E_{ad}$ with the change of density ratio of ligands and receptors ρ_L/ρ_R, for $\bar\kappa_n = 1$, $\bar\sigma = 0.1$, $\bar\gamma = 10$, and $\bar e_{RL} = 35$. It can be seen from Fig. 2 that the ligand density can significantly influence the wrapping process, as indicated by the variations of the energy and wrapping degree. As expected,

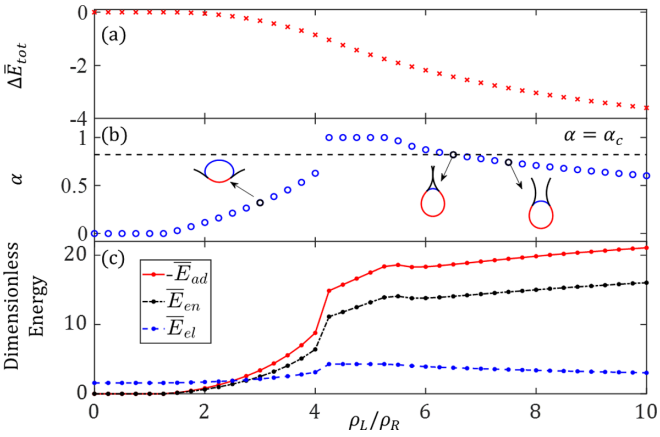

FIG. 2. (a) The dimensionless energy change, (b) wrapping degree, and (c) three energy components as functions of dimensionless ligand density, ρ_L/ρ_R, for $\bar{\kappa}_n = 1$, $\bar{\sigma} = 0.1$, $\rho_R = 0.1$, $\bar{\gamma} = 10$, and $\bar{e}_{RL} = 35$. As presented in (b), three characteristic wrapping profiles are marked by the three black circles.

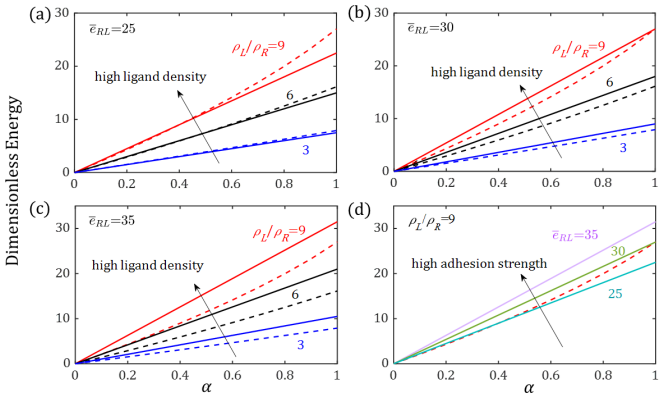

FIG. 3. Comparisons of the minus adhesion energy $-\bar{E}_{ad}$ (solid lines) and entropy contribution to the free energy $\bar{E}_{en}$ (dashed lines) in dimensionless forms as functions of the wrapping degree for $\rho_L = 3\rho_R,\ 6\rho_R,\ 9\rho_R$, $\bar{\gamma} = 10$ and (a) $\bar{e}_{RL} = 25$, (b) $\bar{e}_{RL} = 30$, and (c) $\bar{e}_{RL} = 35$, respectively. (d) Comparisons of the minus adhesion energy $-\bar{E}_{ad}$ (solid lines) and entropy contribution to the free energy $\bar{E}_{en}$ (dashed line) in dimensionless forms as functions of the wrapping degree for $\bar{e}_{RL} = 25,\ 30,\ 35$, $\rho_L = 9\rho_R$.

the energy change $\Delta\bar{E}_{\rm tot}$ decreases monotonically as the ligand density increases, which implies that the higher the ligand density, the more stable the state of NP wrapping becomes. In the limit of $\rho_L/\rho_R \to 0$, we have $\Delta\bar{E}_{\rm tot} \to 0$, which means that the vesicle NP can no longer adhere to the membrane due to the shortage of ligands as reported in a previous paper [9].

Figure 2(b) shows the variation of the wrapping degree along with the ligand density. We can see that the wrapping degree firstly increases along with ρ_L/ρ_R, and reaches its critical value α_c, as $\rho_L/\rho_R = 4.25$, at which membrane sections on both sides of the vesicle NP start to make contact, to enclose the vesicle NP. As ρ_L/ρ_R further increases, by neglecting the excluded volume effect, the wrapping degree will continue to increase, then stays at $\alpha = 1$ for $\rho_L/\rho_R \in [4.25, 5.25]$, and eventually drops as $\rho_L/\rho_R = 5.25$ due to the increase of the entropic contribution to the energy. Interestingly, there exists a range of the ligand density, $\rho_L/\rho_R \in [4.25, 5.25]$, $\rho_R = 0.1$, within which the wrapping degree reaches its maximum value, $\alpha = 1$. Although α will not reach 1 when the excluded volume effect is taken into account, this region with $\alpha = 1$ in Fig. 2(b) still shows that the adhesion energy, as the energy component to drive the wrapping process, is dominant when compared with the energy of the entropy contribution. We can imagine that this region tends to form an enclosed adhesion, but it may need the assistance of membrane fusion in the actual process. This finding seems consistent with previous experimental observations [29–34] that NPs with a certain range of ligand density can be more easily encapsulated than those with out of range ligand density. The existence of the range of $\rho_L/\rho_R \in [4.25, 5.25]$ with the enclosed state of wrapping is mainly induced by the competition between the favorable energy (binding energy) and the unfavorable energy (elastic energy and energy of the entropy contribution). When the ligand density is too small, the binding energy of receptor-ligand bonds becomes insufficient to deform the elastic cell membrane and the NP, which is known as phenomenon of ligand shortage [9]. On the other hand, when the ligand density of the NP is large, the rapid entropy change of the distributed receptors would consume most favorable receptor-ligand binding energy; thus the cellular uptake of the vesicle NP is less likely to occur at high ligand density. The smaller the receptor density on the cell membrane, the more intensive the energy of the entropy contribution. Therefore, the high ligand density on the NP results in another regime of receptor shortage. For the case that the receptor density is comparable to that of the ligands, the receptors can barely diffuse to the binding sites and the resistance to the wrapping process is dominated by elastic deformations of the membrane and the vesicle NP.

Meanwhile, Fig. 2(c) shows a comparison of the energy of the entropy contribution, elastic energy, and minus adhesion energy as functions of the dimensionless ligand density. We can observe from Fig. 2(c) that the value of the energy of the entropy contribution is larger than that of the elastic energy at high ligand density.

Figure 3 displays a comparison of the favorable adhesion energy of the receptor-ligand complex and the unfavorable energy of change in entropy of the receptors as a function of the wrapping degree for $\bar{e}_{RL} = 25,\ 30,\ 35$ and different ligand density $\rho_L = 3\rho_R,\ 6\rho_R,\ 9\rho_R$. One can observe that the absolute values of both adhesion energy and entropic energy increase monotonically with the wrapping degree. Based on Eqs. (6)–(8), the relationship between adhesion energy and the wrapping degree is linear. However, the energy of the entropy contribution exhibits a nonlinear dependency of the wrapping degree. We can see from Fig. 3 that the entropic contribution to the free energy is comparable in quantity to the adhesion energy, and both of them are significantly regulated by the ligand density. More importantly, the higher ligand density induces both the larger adhesion energy and the larger energy of the entropy contribution. This fact suggests that ligand density is an important factor in regulating the cellular uptake process by inducing competition between favorable adhesion energy and unfavorable energy of the entropy contribution.

We have investigated how the ligand density and adhesion strength of a single receptor-ligand complex may jointly

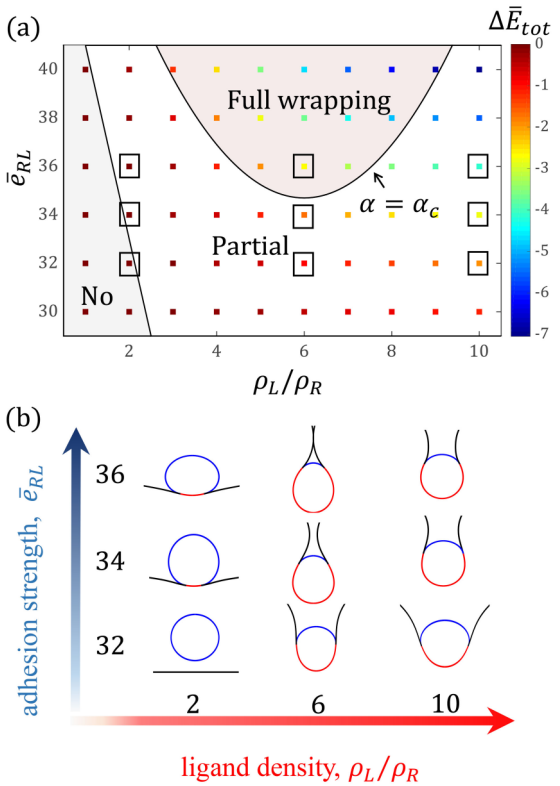

FIG. 4. For $\bar{\kappa}_n = 1$, $\bar{\sigma} = 0.1$, and $\bar{\gamma} = 10$, (a) a two-dimensional phase diagram characterizes the effect of the ligand density and the adhesion strength of a single receptor-ligand complex on the total energy difference. The black solid lines stand for the boundaries between no wrapping, partial wrapping, and full wrapping phases. The black rectangular rings note the selective wrapping states. (b) The corresponding wrapping profiles of nine selective wrapping states in (a).

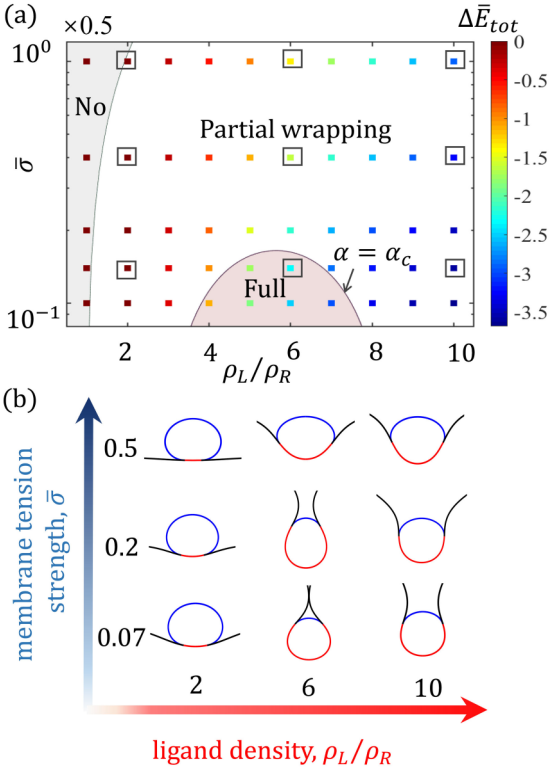

FIG. 5. For $\bar{\kappa}_n = 1$, $\bar{\gamma} = 10$, and $\bar{e}_{RL} = 35$, (a) the dimensionless total energy change as a function of the dimensionless membrane tension and ligand density. The black solid lines are the boundaries between phases of no wrapping, partial wrapping, and full wrapping. Nine typical wrapping states are marked by the black hollow squares. (b) Profiles of the nine marked wrapping states for different membrane tension, strength of the single bond, and ligand density.

affect the cellular uptake behaviors of the vesicle NP. Figure 4 shows the wrapping degree, the free energy change, and phase diagrams that characterize three phases of NP uptake, no wrapping ($\alpha = 0$), partial wrapping ($0 < \alpha < \alpha_c$), and full wrapping ($\alpha_c \leqslant \alpha \leqslant 1$), in terms of the ligand density and binding energy, when $\bar{\kappa}_n = 1$, $\bar{\sigma} = 0.1$, and $\bar{\gamma} = 10$. Note that α_c corresponds to the wrapping state that the membrane sections on both sides of the vesicle NP just get to contact. Then the full wrapping with $\alpha_c \leqslant \alpha \leqslant 1$, which is numerically obtained by omitting the excluded volume effect of the membrane, refers to the state where the vesicle NP is fully enclosed by the membrane. For the case in Fig. 4, we have determined the critical wrapping degree as $\alpha_c = 0.82$.

In order to more intuitively understand how the event of NP uptake depends on the binding energy of each single receptor-ligand bond and ligand density, typical wrapping profiles at $\bar{\kappa}_n = 1$, $\bar{\sigma} = 0.1$, and $\bar{\gamma} = 10$ for different ligand density and binding energy have been studied and illustrated in Fig. 4(b) [in this paper the wrapping profiles of full wrapping ($\alpha_c \leqslant \alpha \leqslant 1$) are depicted by the case where the membrane sections on both sides of the vesicle NP just get to contact]. We can see that the wrapping phase is significantly affected by the ligand density. Moreover, as shown in Fig. 4(a), for the binding strength $\bar{e}_{RL}$ ranging from 30 to 40, the transition of the wrapping phases is obvious when the intermediate value of ligand density is taken and rarely takes place in both the regions of small ligand density (ligand shortage regime) and high ligand density (receptor shortage regime).

In addition to the binding energy of single receptor-ligand bond, we also examine the effect of ligand density on the uptake behaviors for different tension strengths of membrane as displayed in Fig. 5. Three different wrapping phases are shown in Fig. 5(a), where the numerically determined critical wrapping degree α_c ranges from 0.78 to 0.89 with the variation of membrane tension strength. We can see from Fig. 5(a) that the wrapping degree decreases, and the total energy increases with the increasing membrane tension. Meanwhile, for a given membrane tension, there also exists an optimal ligand density for the maximum wrapping degree. Typical wrapping profiles are plotted in Fig. 5(b). The dependence of the wrapping phase on the ligand density can also be clearly observed under different strengths of membrane tension.

As shown in Appendix A, a valid range of λ has been estimated as roughly 5–20. Within this range, a series of ρ_R around 0.1 is adopted to find the dependency of the existence of optimal ligand density on different combinations of $\lambda - \rho_R$. Figure 6 shows that the optimal ligand density exists in most of the cases. However, in the case of large receptor density and length ratio, there will be dense receptors distributed on

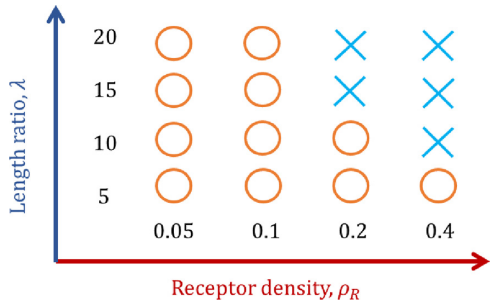

FIG. 6. A two-dimensional phase diagram on the $\lambda - \rho_R$ plane characterizes the interrelated effect of length ratio between the lipid membrane and vesicle contour, and receptor density on the wrapping uptake for $\bar{\kappa}_n = 1$, $\bar{\sigma} = 0.1$. The hollow circles represent the existence of optimal ligand density for the maximum wrapping degree, and the crossings represent the nonexistence of such optimal values of ligand density. In order to investigate how the length ratio and receptor density may affect the optimal ligand density, we have considered $\bar{\gamma}$ and $\bar{e}_{RL}$ as two free parameters.

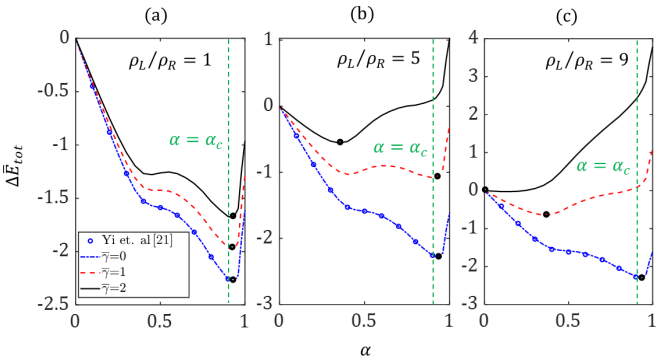

FIG. 8. The energy change as a function of wrapping degree for $\bar{\kappa}_n = 0.1$, $\bar{\sigma} = 0.075$, and different ligand densities (a) $\rho_L/\rho_R = 1$, (b) $\rho_L/\rho_R = 5$, and (c) $\rho_L/\rho_R = 9$. The adhesion energy density is kept constant, $\rho_L\bar{e}_{RL} = 1.5\pi$, although entropy-related energy is considered. The black circles represent the wrapping degrees that are associated with the minimum free energy. To have a fair comparison between the present statistical mechanics model and the previous elastic model [21], all relevant parameters are taken from Ref. [21].

the cell membrane, which increases the number of distribution configurations of receptors. Then the entropic contribution to the free energy becomes negligible; the membrane and the vesicle deformation will play the dominant role in resistance to the wrapping uptake as reported in previous papers [21,44,46,52]. For such a case, the optimal ligand density no longer exists, as shown in Fig. 6.

Previous studies have demonstrated that rigidity of NPs can influence their cellular uptake [21,22,52,53]. Figure 7 shows the wrapping degree associated with the state of minimum free energy as a function of the ratio of the bending stiffness of the lipid membrane and the vesicle NP for different ligand densities. One can see from Fig. 7 that the vesicles tend to be completely enveloped by the cell as they become stiffer and the fully wrapping states [$\bar{\kappa}_n = 10$ or 20, shown in Fig. 7(a)] can occur for the stiffer NP rather than the softer one with the high ligand density. The reason is that the adhesion energy is not large enough to overcome the energy barrier of

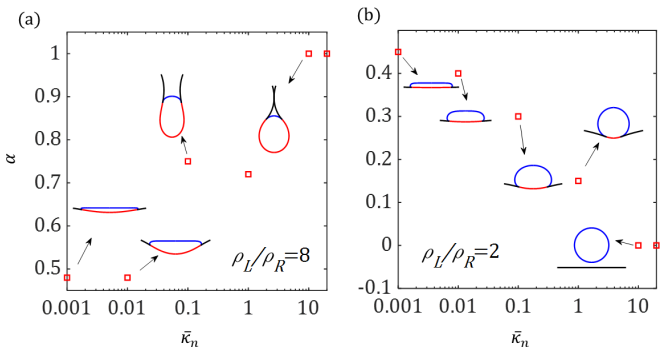

FIG. 7. The wrapping degree as a function of the ratio of the bending stiffness of the lipid membrane and the vesicle NP for $\bar{\sigma} = 0.1$, $\bar{e}_{RL} = 35$, and $\bar{\gamma} = 10$, in variation with (a) high ligand density, $\rho_L = 8\rho_R$, and (b) low ligand density, $\rho_L = 2\rho_R$, respectively. Here, for full wrapping ($\alpha_c \leqslant \alpha \leqslant 1$), the associated wrapping profile is schematically displayed by the case that the membrane sections on both sides of the vesicle NP just get to contact.

deformation across the semiencapsulated state of the soft NP. These observations are accordant with the previous studies on the so-called rigidity-dependent cellular uptake [21,22,52,53]. However, for a relatively small ligand density, although both of the soft and stiff NPs cannot be completely encapsulated by the membrane, the softer one is more likely to firmly adhere to the membrane than the stiffer one, as stiff NPs are hard to deform, which reduces the contact area of the NP-membrane system and then the formation probability of receptor-ligand bonds. This finding indicates that the ligand density plays a comparable role as the stiffness on mediating cellular uptake of NPs.

To further examine the entropic effect on the cellular uptake of NPs, Fig. 8 shows the evolution of the change in total energy along with the wrapping degree under different entropy strengths and ligand densities. For the reduced case of zero entropy strength, our model can be completely degenerated to previous models of elastic membrane wrapping of elastic or rigid NPs [21,44,52,54,55], in which the uptake process is considered to be only regulated by the elastic deformation of the NP-membrane system. It can be seen from Fig. 8 that the wrapping degrees associated with the minimum free energy calculated from our model with consideration of entropic contribution are highly consistent with the result from the previous elastic model [21] at low ligand density. However, with the increase of ligand density, the determined wrapping degree associated with the minimum free energy distinctly decreases. The underlying reason is that sharp change in the configuration of distributed receptors before and after NP-cell interaction will significantly dissipate the favorable binding energy in the case of high ligand density. As shown in Fig. 8(a), there actually exist multiple metastable states of NP wrapping. Similar phenomena have been reported in [21] without considering entropic effect. In this study, we have mainly focused on the wrapping state associated with the minimum free energy. It is very common that the interaction between deformable NPs and living cells usually occurs in a fluctuation-sensitive biological environment [56–59]. Under

such a situation, the wrapping states of the NPs may stochastically switch between these multiple metastable states due to the thermal fluctuations of the membrane, the NP, and the adhesion molecules, etc.

It is also worth noting that the isssue of two fluctuating membranes interacting via receptor-ligand bonds has been theretically and computationally addressed [37–39]. Due to an infinite reservoir of receptors and ligands being considered, the monotonically increasing relationship between the effective adhesion potential and the overall concentration of receptors and ligands is predicted [37–39]. Nevertheless, as a vesicle NP interacting with a finite membrane is considered in the current context, the finite reservoir of receptors would decrease the effective adhesion potential at high ligand density, resulting in a nonmonotonic relationship between the effective adhesion potential and the overall concentration of receptors. Accordingly, the depletion of receptors from the finite reservoir leads to optimum ligand density with maximum wrapping degree of NP.

IV. CONCLUSION

In summary, we have established a theoretical model on the wrapping of a vesicle NP by a finite lipid membrane via formation of ligand-receptor bonds, to investigate the influence of ligand density on cellular uptake of NP. This model quantitatively couples the elastic deformation of the lipid membrane and vesicle, and the statistical mechanics behavior of adhesion molecules. Through sequential quadratic programming, we have numerically calculated the morphologies of the lipid membrane and the vesicle NP associated with the state of minimum free energy. Results reveal that the wrapping behavior significantly depends on the ligand density. As a result of energy competition, an optimal ligand density exists with intermediate value corresponding to the maximum NP wrapping degree. The finding on the dependency of the wrapping state on the ligand density is consistent with the experimental observations of cellular uptake of NPs [29–34]. Three wrapping phases (no wrapping, partial wrapping, and full wrapping) are also systematically identified in terms of the ligand density and the binding strength of the ligand-receptor bond, as well as the membrane tension strength. All these findings may not only shed light on the influence of ligand density on the statistical mechanics behaviors of cellular uptake of NPs, but also may provide guidelines to improve the efficiency of NP-based drug delivery systems.

However, for real systems of cellular uptake of NPs, the proposed model still has the following limitations. Influences of ligand diffusion, membrane fluctuation, coexistence of different types of receptors and ligands, and remodeling in the cell cortex, etc., are not taken into account. Actually, the choice of a finite membrane with limited receptors and the assumption that all ligands are bound with receptors one by one will amplify the entropy cost. A 2D model is adopted in this study. Although some conclusions are generic and can be safely extrapolated to the three-dimensional (3D) case, deformations in 2D can still be quite different from a real 3D system. Investigation into the effects of these factors on cellular uptake of NPs requires a more sophisticated model and would be considered for our future work.

ACKNOWLEDGMENTS

This study is supported by grants from the National Natural Science Foundation of China (Grants No. 11925204 and No. 12072137) and the Open Fund of Key Laboratory for Intelligent Nano Materials and Devices of the Ministry of Education NJ2020003 (Grant No. INMD-2021M03). The authors would like to thank the anonymous referees for their comprehensive and constructive comments.

APPENDIX A: ESTIMATION ON THE EFFECTIVE SIZE OF CELL MEMBRANE

It has been generally accepted that endocytosis of viruses by cells is associated with the deformation of the membrane and the diffusion of adhesion molecules on the membrane surface. When a virus particle makes contact with a target cell, we assume that only a finite area of the cell membrane may affect the endocytosis process. We consider an effective size of cell membrane, $2l_m$, which is assumed to be large enough compared to that of the virus. In addition, most viruses are spherical and show a characteristic radius R in the range of 10–100 nm [60,61]. The actual time t_w required for viruses to enter a cell is revealed as 0.01–1 s by force tracing based on atomic force microscopy [62–64]. Within this wrapping time, we further assume that, in the membrane with such an effective size, the farthest receptor should be supposed to be just able to reach the contact area of the virus and membrane. Thus, with this restriction, the average value of the effective size of the cell membrane can be roughly estimated as

$$l_m \sim \sqrt{4Dt_w}, \tag{A1}$$

where D denotes the diffusion coefficient of receptors on the cell membrane and its value ranges from 0.01 to 10 $\mu\mathrm{m}^2/\mathrm{s}$ as reported in a large number of reports [65–76]. Then, the ratio between this effective size and the contour size of the virus can be given as

$$\lambda = \frac{l_m}{\pi R}. \tag{A2}$$

Although the previous study has indicated that there is an optimal size for the virus to be absorbed by the cell, a trend of positive correlation between the wrapping time and the size of the virus in general can still be found [7] under certain circumstances. Following this relationship that the maximum and minimum size correspond to the maximum and minimum wrapping time, the ratio λ can be roughly estimated as between 0.6 and 20. The lower and upper limits of λ result from two extreme cases of slow ($D = 0.01$ $\mu\mathrm{m}^2/\mathrm{s}$) and fast ($D = 10$ $\mu\mathrm{m}^2/\mathrm{s}$) diffusion of adhesion molecules, respectively. On the other hand, we should avoid introducing the artificial boundary effect during the wrapping process in the model; therefore, the ratio λ cannot be set too small. As has been verified by our numerical results and previous study [21], the ratio λ should be, at least, larger than about 5; then the boundary deformation of the membrane will almost not be affected by the wrapping. Eventually, the range of possible λ can be narrowed to roughly 5–20.

In particular, when typical values of R, t_w, and D are adopted as 50 nm [77–80], 0.3 s [24,62], and 2 $\mu m^2/s$, the ratio λ can be readily estimated as $\sim$10.

On the other hand, as one of the well-known viruses, HIVs have been deeply studied in recent years. The HIV particles ($R \sim 50$ nm [80]) are usually coated with about 70 spikes [81]. The CD4+ T cells are white blood cells that the HIV virus kills. The CD4+ T cell usually shows a typical circular shape and is 6–10 μm in diameter [82]. It has also been demonstrated that the number of CD4 receptors, which are known as the primary receptors on the surfaces of the CD4+ T cells for HIV infection, is at a mean level of 46 000 receptors per cell [83]. Such amount of receptors can allow a CD4+ T cell, at most, to completely encapsulate about 657 HIV viruses at the same time. Interestingly the average membrane area occupied by each viral particle is about 30 000 nm^2 which is about 10 times the surface area of the HIV viral particle.

Given the above, the ratio $\lambda \sim 10$ is adopted in our study.

APPENDIX B: ESTIMATION ON THE DIMENSIONLESS RECEPTOR DENSITY

As one of the well-known viruses, HIV has been deeply studied in recent years. For an HIV particle ($R \sim 50$ nm [80]) coated with about 70 spikes [81], the ligand density can be roughly calculated as $\sim 2200/\mu m^2$. Each CD4+ T cell usually has a mean level of 46 000 receptors [82] for HIV infection. In addition, the CD4+ cells usually show a typical circular shape with diameter 6–10 μm [83]. The receptor density on the cell surface can be estimated as $\sim 300/\mu m^2$.

Because a 2D model is considered to describe a NP's interaction with a lipid membrane in this study, for consistency, we will consider to apply line number density (ξ) instead of the area density (χ) to describe the distribution of adhesion molecules along the NP and the membrane. The line number density can be related to the area density by the equation $\xi = \sqrt{\chi}$. This relation can also be understood as that the line number density ξ is determined as the area density χ multiplied by the mean molecule distance, $\sqrt{1/\chi}$ [84].

Based on this, the ligand density of the HIV virus and the corresponding receptor density on CD4+ T cell can be given as

$$\xi_L \sim 0.05/\text{nm}, \tag{B1}$$

$$\xi_R \sim \frac{0.02}{\text{nm}}, \tag{B2}$$

where ξ_L and ξ_R represent the ligand density along the NP and the receptor density along the lipid membrane, respectively.

In addition, considering the minimum ligand spacing is about 5 nm [36], the density of the maximum permissible sites on the cell for receptors can be estimated as

$$\xi_T \sim 0.2/\text{nm}. \tag{B3}$$

Thus, the dimensionless ligand and receptor densities for the HIV particle can be determined as

$$\rho_L = \frac{\xi_L}{\xi_T} \sim 0.25 \tag{B4}$$

and

$$\rho_R = \frac{\xi_R}{\xi_T} \sim 0.1. \tag{B5}$$

Based on the analysis of the HIV particle, $\rho_R = 0.1$ is adopted in our paper.

[1] C. A. Poland, R. Duffin, I. Kinloch, W. A. Maynard, A. Wallace, A. Seaton, V. Stone, S. Brown, W. Macnee, and K. Donaldson, Nat. Nanotechnol. **3**, 423 (2008).

[2] G. Sahay, D. Y. Alakhova, and A. V. Kabanov, J. Controlled Release **145**, 182 (2010).

[3] R. A. Petros and J. M. Desimone, Nat. Rev. Drug Discovery **9**, 615 (2010).

[4] M. E. Davis, Z. G. Chen, and D. M. Shin, Nat. Rev. Drug Discovery **7**, 771 (2008).

[5] P. Decuzzi, ACS Nano **10**, 8133 (2016).

[6] G. Bao, Y. Bazilevs, J. H. Chung, P. Decuzzi, H. D. Espinosa, M. Ferrari, H. Gao, S. S. Hossain, T. J. Hughes, and R. D. Kamm, J. R. Soc., Interface **11**, 3834 (2014).

[7] H. Gao, W. Shi, and L. B. Freund, Proc. Natl. Acad. Sci. USA **102**, 9469 (2005).

[8] S. Zhang, J. Li, G. Lykotrafitis, G. Bao, and S. Suresh, Adv. Mater. **21**, 419 (2009).

[9] H. Yuan, J. Li, G. Bao, and S. Zhang, Phys. Rev. Lett. **105**, 138101 (2010).

[10] A. Xu, M. Yao, G. Xu, J. Ying, W. Ma, B. Li, and Y. Jin, Int. J. Nanomed. **7**, 3547 (2012).

[11] S. Dasgupta, T. Auth, and G. Gompper, Nano Lett. **14**, 687 (2014).

[12] W. Shi, J. Wang, X. Fan, and H. Gao, Phys. Rev. E **78**, 061914 (2008).

[13] P. Decuzzi and M. Ferrari, Biophys. J. **94**, 3790 (2008).

[14] D. M. Richards and R. G. Endres, Proc. Natl. Acad. Sci. USA **113**, 6113 (2016).

[15] R. Vácha, F. J. Martinez-Veracoechea, and D. Frenkel, Nano Lett. **11**, 5391 (2011).

[16] A. H. Bahrami, Soft Matter **9**, 8642 (2013).

[17] X. Shi, A. von Dem Bussche, R. H. Hurt, A. B. Kane, and H. Gao, Nat. Nanotechnol. **6**, 714 (2011).

[18] J. Wang and L. Li, J. R. Soc., Interface **12**, 20141023 (2015).

[19] C. Huang, Y. Zhang, H. Yuan, H. Gao, and S. Zhang, Nano Lett. **13**, 4546 (2013).

[20] X. Yi and H. Gao, Soft Matter **11**, 1107 (2015).

[21] X. Yi, X. Shi, and H. Gao, Phys. Rev. Lett. **107**, 098101 (2011).

[22] J. Sun, L. Zhang, J. Wang, Q. Feng, D. Liu, Q. Yin, D. Xu, Y. Wei, B. Ding, and X. Shi, Adv. Mater. **27**, 1402 (2015).

[23] J. Wang, L. Li, and Y. Zhou, Chin. Sci. Bull. **59**, 2277 (2014).

[24] L. Li, Y. Zhang, and J. Wang, Europhys. Lett. **124**, 48002 (2018).
[25] H. M. Ding and Y. Q. Ma, Small **11**, 1055 (2015).
[26] H. Gao, J. Mech. Phys. Solids **62**, 312 (2014).
[27] V. Schubertová, F. J. Martinez-Veracoechea, and R. Vácha, Soft Matter **11**, 2726 (2015).
[28] L. Li, Y. Zhang, and J. Wang, R. Soc. Open Sci. **4**, 170063 (2017).
[29] Y. Shen, J. Chen, Q. Liu, C. Feng, X. Gao, L. Wang, Q. Zhang, and X. Jiang, Int. J. Pharm. **413**, 184 (2011).
[30] D. R. Elias, A. Poloukhtine, V. Popik, and A. Tsourkas, Nanomedicine **9**, 194 (2013).
[31] B. J. Zern, A. M. Chacko, J. Liu, C. F. Greineder, E. R. Blankemeyer, R. Radhakrishnan, and V. Muzykantov, ACS nano **7**, 2461 (2013).
[32] S. Chu, C. Tang, and C. Yin, Biomaterials **52**, 229 (2015).
[33] A. Bandyopadhyay, R. L. Fine, S. Demento, L. K. Bockenstedt, and T. M. Fahmy, Biomaterials **32**, 3094 (2011).
[34] A. M. Alkilany, L. Zhu, H. Weller, A. Mews, W. Parak, M. Barz, and N. Feliu, Adv. Drug Delivery Rev. **143**, 22 (2019).
[35] A. S. Smith and U. Seifert, Phys. Rev. E **71**, 061902 (2005).
[36] W. Helfrich, Z. Naturforsch., C **28**, 693 (1973).
[37] H. Krobath, B. Różycki, R. Lipowsky, and T. R. Weikl, Soft Matter **5**, 3354 (2009).
[38] B. Różycki, R. Lipowsky, and T. R. Weikl, New J. Phys. **12**, 095003 (2010).
[39] T. R. Weikl and R. Lipowsky, Phys. Rev. E **64**, 011903 (2001).
[40] R. Lipowsky, Nature (London) **349**, 475 (1991).
[41] X. Yi and H. Gao, Phys. Rev. E **89**, 062712 (2014).
[42] S. Mkrtchyan, C. Ing, and J. Z. Y. Chen, Phys. Rev. E **81**, 011904 (2010).
[43] T. R. Weikl, Eur. Phys. J. E **12**, 265 (2003).
[44] H. Tang, H. Ye, H. Zhang, and Y. Zhang, Soft Matter **11**, 8674 (2015).
[45] K. A. Dill and S. Bromberg, *Molecular Driving Forces: Statistical Thermodynamics in Chemistry and Biology* (Garland Science, New York, 2011).
[46] J. Wang, H. Yao, and X. Shi, J. Mech. Phys. Solids **73**, 151 (2014).
[47] M. Deserno, Phys. Rev. E **69**, 031903 (2004).
[48] W. T. Góźdź, J. Phys. Chem. B **109**, 21145 (2005).
[49] W. T. Góźdź, Langmuir **23**, 5665 (2007).
[50] H. G. Döbereiner, E. Evans, M. Kraus, U. Seifert, and M. Wortis, Phys. Rev. E **55**, 4458 (1997).
[51] J. Nocedal and S. Wright, *Numerical Optimization* (Springer, New York, 2006).
[52] M. Raatz, R. Lipowsky, and T. R. Weikl, Soft Matter **10**, 3570 (2014).
[53] P. Guo, D. Liu, K. Subramanyam, B. Wang, J. Yang, J. Huang, D. T. Auguste, and M. A. Moses, Nat. Commun. **9**, 130 (2018).
[54] A. H. Bahrami, M. Raatz, J. Agudo-Canalejo, R. Michel, E. M. Curtis, C. K. Hall, and T. R. Weikl, Adv. Colloid Interface Sci. **208**, 214 (2014).
[55] M. Deserno and T. Bickel, Europhys. Lett. **62**, 767 (2003).
[56] S. F. Fenz, T. Bihr, D. Schmidt, R. Merkel, U. Seifert, K. Sengupta, and A. S. Smith, Nat. Phys. **13**, 906 (2017).
[57] W. Bialek and W. Bialek, *Biophysics: Searching for Principles* (Princeton University, Princeton, NJ, 2012).
[58] P. Nelson, *Biological Physics: Energy, Information, Life* (Freeman, New York, 2003).
[59] F. Frey, F. Ziebert, and U. S. Schwarz, Phys. Rev. Lett. **122**, 088102 (2019).
[60] A. J. Cann, *Principles of Molecular Virology* (Academic Press, San Diego, CA, 2001).
[61] J. A. Levy, H. F. Fraenkel-Conrat, and R. A. Owens, *Virology* (Prentice-Hall, New York, 1994).
[62] Y. Pan, F. Zhang, L. Zhang, S. Liu, M. Cai, Y. Shan, and H. Wang, Adv. Sci. **4**, 1600489 (2017).
[63] Y. Pan, S. Wang, Y. Shan, D. Zhang, J. Gao, M. Zhang, and Q. Qin, Small **11**, 2782 (2015).
[64] R. Wang, X. Yang, D. Leng, Q. Zhang, D. Lu, S. Zhou, and Y. Shan, Anal. Methods **11**, 1724 (2019).
[65] O. M. Szklarczyk, N. González-Segredo, P. Kukura, A. Oppenheim, D. Choquet, V. Sandoghdar, A. Helenius, I. F. Sbalzarini, and H. Ewers, PLoS Comput. Biol. **9**, e1003310 (2013).
[66] O. Thoumine, E. Saint-Michel, C. Dequidt, J. Falk, R. Rudge, T. Galli, C. Faivre-Sarrailh, and D. Choquet, Biophys. J. **89**, L40 (2015).
[67] W. Liu, T. Meckel, P. Tolar, H. W. Sohn, and S. K. Pierce, J. Exp. Med. **207**, 1095 (2010).
[68] B. Favier, N. J. Burroughs, L. Wedderburn, and S. Valitutti, Int. J. Immunol. **13**, 1525 (2001).
[69] S. Ramadurai, A. Holt, V. Krasnikov, G. van den Bogaart, J. A. Killian, and B. Poolman, J. Am. Chem. Soc. **131**, 12650 (2009).
[70] S. Ramadurai, R. Duurkens, V. V. Krasnikov, and B. Poolman, Biophys. J. **99**, 1482 (2010).
[71] R. Worch, Z. Petrášek, P. Schwille, and T. Weidemann, J. Membrane Biol. **250**, 393 (2017).
[72] B. L. Sprague, F. Müller, R. L. Pego, P. M. Bungay, D. A. Stavreva, and J. G. McNally, Biophys. J. **91**, 1169 (2006).
[73] D. Choquet and A. Triller, Nat. Rev. Neurosci. **4**, 251 (2003).
[74] M. Triantafilou, S. Morath, A. Mackie, T. Hartung, and K. Triantafilou, J. Cell Sci. **117**, 4007 (2004).
[75] M. Dahan, S. Levi, C. Luccardini, P. Rostaing, B. Riveau, and A. Triller, Science **302**, 442 (2003).
[76] R. L. Yauch, R. L. Felsenfeld, S. K. Kraeft, L. B. Chen, M. P. Sheetz, and M. E. Hemler, J. Exp. Med. **186**, 1347 (1997).
[77] V. Monteil, H. Kwon, P. Prado, A. Hagelkrüys, R. A. Wimmer, M. Stahl, J. P. Romero *et al.*, Cell **181**, 905 (2020).
[78] A. L. Katzenstein and F. B. Askin, *Infection* (W. B. Saunders Company, Philadelphia, 1990).
[79] R. E. F. Matthews, Intervirology **11**, 133 (1979).
[80] R. Ramalho, S. Rankovic, J. Zhou, C. Aiken, and I. Rousso, Retrovirology **13**, 17 (2016).
[81] P. Zhu, J. Liu, J. Bess, E. Chertova, J. D. Lifson, H. Grisé, and K. H. Roux, Nature (London) **441**, 847 (2006).
[82] D. Rossi, D. Dannhauser, M. Telesco, P. Nettiab, and F. Causa, Lab Chip **19**, 3888 (2019).
[83] P. Poncelet, G. Poinas, P. Corbeau, C. Devaux, N. Tubiana, N. Muloko, and J. Sampol, Res. Immunol. **142**, 291 (1991).
[84] J. Qian, J. Wang, and H. Gao, Langmiur **24**, 1262 (2008).